C. R. Palevol 9 (2010) 435–443

Contents lists available at ScienceDirect

Comptes Rendus Palevol

www.sciencedirect.com

General palaeontology

# Calvarial shape variation among Middle Pleistocene hominins: An application of surface scanning in palaeoanthropology

## *Les variations de conformation du calvarium durant le Pléistocène moyen : une application de scan surfacique en paléoanthropologie*

Martin Friess

*Département Hommes, Natures, Sociétés, CNRS, UMR 7206, 43, rue Buffon, 75013 Paris, France*

ARTICLE INFO

*Article history:*
Received 28 February 2010
Accepted after revision 30 July 2010
Available online 28 September 2010

Written on invitation of the Editorial Board

*Keywords:*
3D surface scanning
Geometric morphometrics
Neandertals
*Homo heidelbergensis*
*Homo rhodesiensis*
Middle Pleistocene

ABSTRACT

The increasing availability of 3D data and tools offers new analytical perspectives in palaeoanthropology, such as the quantitative testing of opposing phylogenetic scenarios. Using optical surface scan data and geometric morphometric techniques, this study explores calvarial shape variation in the "Middle Pleistocene muddle". The morphological variability between *H. erectus* on the one hand and *H. sapiens*/*neanderthalensis* on the other has long remained obscure: opposing views have attributed the known specimens to any of the three species and possibly one or two more. A large number of landmarks and semilandmarks was extracted from the braincase and the face, in order to quantify the calvarial shape differences among species and key fossils. The results are incompatible with the hypothesis that *H. rhodesiensis* is the exclusive ancestor of *H. sapiens*, and offer only weak support for an exclusively European ancestor of Neandertals.



*Mots clés :*
Scan 3D surfacique
Morphométrie géométrique
Néandertal
*Homo heidelbergensis*
*Homo rhodesiensis*
Pléistocene moyen

RÉSUMÉ

Le nombre de données et d'outils tridimensionnels étant en augmentation permanente, ceux-ci offrent de nouvelles perspectives en paléoanthropologie, comme le test de scénarios évolutifs opposés. En utilisant des données issues d'un *scan* optique, et en les analysant par la morphométrie géométrique, cette étude explore les variations de conformation calvariale durant la « confusion du Pléistocène moyen ». En effet, la variabilité morphologique entre *H. erectus* et *H. sapiens*/*neanderthalensis*, est longtemps restée obscure, si bien que des spécimens fossiles ont été attribués à l'une ou l'autre espèce, et parfois même à d'autres espèces. Un grand nombre de *landmarks* et *semi-landmarks* a été enregistré, afin de quantifier les différences du calvarium entre espèces et spécimens. Les résultats sont incompatibles avec la notion de *H. rhodesiensis* comme ancêtre exclusif de *H. sapiens*, et fournissent un faible soutien à un ancêtre exclusivement européen des Néandertaliens.



## 1. Introduction

Palaeoanthropological research has greatly benefited in recent years from advances in 3D imaging and quanti-

*E-mail addresses:* friess@mnhn.fr, mf@martinfriess.com.

1631-0683/$ – see front matter © 2010 Académie des sciences. Published by Elsevier Masson SAS. All rights reserved.
doi:10.1016/j.crpv.2010.07.016

tative analysis. While medical or micro-CT scanning are among the more frequently used techniques to acquire 3D data, their implementation and practical application still remains relatively confined due to technical requirements resulting from radiation, required computing power for large data sets, as well as limited access and mobility. Given these constraints and their associated cost, non-radiating surface scanning has become a convenient alternative for studies of external morphology (Friess, 2006; Friess et al., 2002; Harcourt-Smith et al., 2008; Lyons et al., 2000; Tocheri et al., 2005). Surface scanners operate in the visible light spectrum, yielding optical resolutions anywhere between 1 mm and several microns, which is potentially higher than that of standard medical scanning. In addition, most systems are portable, though specifications vary significantly between manufacturers, as does the cost. With the added benefit of being operable without any particular certification or caution (pertaining to radiation), the spreading success, among palaeoanthropologists, of low-cost systems, comes as no surprise.

Analyses of surface scan data, which are acquired without ionizing radiation, typically focus on various measures of surface area, curvatures and volumes, as well as the extraction of linear dimensions and coordinate data. This study explores a more comprehensive use of the very dense point clouds that are surface scans, by applying a geometric morphometric analysis to the surfaces of Middle Pleistocene hominin calvaria. Given the topic of the present volume, this study illustrates how surface scan data can provide additional quantitative insight into a particular issue, which will be exemplified by mid-Pleistocene hominin variation. Another goal is to further improve our understanding of shape variation among these hominins and how it relates to the origin and evolution of Neandertals, a palaeoanthropological issue still waiting to be solved in a definitive manner.

Phylogenetic relationships among Later Pleistocene hominins have been at the center of palaeoanthropology for a very long time. A core issue during the second half of the 20th century has been the role of Neandertals, and in particular their demise and interaction, now seen as fairly limited (Green et al., 2010), with anatomically modern humans. Indeed, as increasing data have been obtained on their phenetic, genetic and behavioral make-up, a majority of scholars now tends to consider them as a separate species, *H. neanderthalensis*, that split from the modern human line, anywhere between 400 and 600 ky bp (Endicott et al., 2010; Hublin, 2009). While this consensus has slowly been settling in, the question of Neandertal origins has resurfaced as a corollary, though answers are still being debated. Several scenarios have been proposed to address both the chronology and phylogeny of what has been referred to as the "muddle in the Middle" Pleistocene (Butzer and Isaac, 1976; Rightmire, 1998). A key question in this context is the recognition of *H. heidelbergensis*, either as exclusively European species or as inclusive of African specimens, namely Kabwe. The main viewpoints are:

- *H. heidelbergensis* is Afro-European. Under this scenario, *H. heidelbergensis* includes specimens from Europe (Sima de los Huesos, Tautavel, Petralona, possibly Steinheim) and Africa (Bodo, Kabwe, Elandsfontein, Salé, Eyasi, Ndutu; Rightmire, 2009; Tattersall, 1992) and is ancestral to both *H. neanderthalensis* and *H. sapiens*;
- *H. heidelbergensis* is exclusively European. Under this scenario, *H. heidelbergensis* is recognized only in Europe, and consequently is ancestral only to, or forms a chronospecies of the Neandertal lineage (Bermúdez de Castro et al., 1997). In this case the taxon includes specimens such as Mauer, Sima de los Huesos (SH), Arago, Bilzingsleben, Vertesszöllös, Petralona, Swanscombe and Steinheim, as well as later "pre-Neandertals" like Biache, and Saccopastore. Furthermore, African large-brained, non-modern skulls are assigned, at least in part, to *H. rhodesiensis*, which is seen as the sole ancestor of *H. sapiens*.

## 2. Using 3D morphometrics to test phylogenetic scenarios

Morphologically, the evolution of anatomically modern *humans* is associated with a more globular braincase and a smaller face that is also more retracted underneath the anterior cranial fossa (Day and Stringer, 1982; Lieberman et al., 2002), while their large-brained predecessors (that is, depending on the author, *H. heidelbergensis*/archaic *H. sapiens*/*H. rhodesiensis*) still retain plesiomorphic resemblance with *H. erectus* (*sensu lato*) through a relatively long and low braincase with strong postorbital constriction, a large, projecting face and less expanded parietals. At the same time, several traits among Neandertals have been described as derived. Among these, and most relevant in terms of calvarial shape, are the increased endocranial volume and associated round shape in posterior view, reduced overall prognathism (both shared with *H. sapiens*), as well as unique features like the marked midfacial prognathism and the presence of an occipital bun. *H. erectus* on the other hand combines largely ancestral features, such as the pentagonal shape of the braincase, or long and low temporal bones with a more angular outline, as opposed to the derived pattern, which is more arched in *H. neanderthalensis* and *H. sapiens* (Dean et al., 1998).

To the extent that these characters are more or less quantifiable, their expression can be assessed and compared statistically, thus serving as a test for the phylogenetic scenarios briefly summarized above. Specifically, the quantification of calvarial shape can help address the following aspects of these evolutionary scenarios:

- do Middle Pleistocene fossil hominins form one or more morphometrically distinct groups, positioned somewhere between *H. erectus sensu lato* on the one hand and and *H. sapiens* on the other?
- is any such intermediate group ancestral only to Neandertals? If so, it should cluster closely with them, but lack the globular shape of *H. sapiens*, and by the same token be distinct from *H. rhodesiensis*. *H. rhodesiensis*, however, should be distinct from both (European) *H. heidelbergensis* and the Neandertal lineage, while exhibiting a more *sapiens*-like, apomorphic skull shape;

- alternatively: Is there a candidate for the role of common ancestor of both Neandertals and *H. sapiens*? If African and European specimens, currently assigned to either *H. rhodesiensis* or *H. heidelbergensis*, cannot be distinguished, and together bridge the morphospace between *H. sapiens*, Neandertals *and H. erectus s.l.,* then this would be an argument in favor of lumping *H. rhodesiensis* and *H. heidelbergensis* into the ancestor of both *H. sapiens* and *H. neanderthalensis* (Hublin, 2009).

The issues raised here have been recognized decades ago, and the palaeoanthropological scrutiny that they have undergone can only be summarily outlined here. The interested reader is referred to recent reviews on current arguments and their extensive bibliographic references (Hublin, 2009; Rightmire, 2009). A key aspect, in my view, of the evolution of mid Pleistocene calvarial shape lies in the nature of the "characters" that have been attributed to the various species, and to *H. sapiens* in particular. Besides qualitative characters (not suitable for shape statistics), the main differences, briefly reviewed above, refer to the overall shape of the skull, proportions of neuro- to viscerocranium, and to the shape of the infraorbital region. The phylogenetic/taxonomic assessment of most Middle Pleistocene fossil specimens is further hampered by their frequent incompleteness, though this is not unique to this question (Hublin, 2009). Finally, some of the features pertain to anatomical areas with relatively large surfaces and relatively few homologous type I landmarks (*sensu* Bookstein, 1991). Hence, they are quite suitable for quantitative analyses that go beyond that of standard landmarks or the distances between them.

## 3. Material and methods

Fossil and modern human skulls were scanned using a Breuckmann Smartscan stereo system (www.Breuckmann.com) with an optical resolution of 0.26 mm. The complete list of specimens is given in Table 1. Because key features discussed in the literature on Middle Pleistocene hominins involve the brain case and the face, this study focuses on calvarial shape variation, and, consequently, only on reasonably well preserved specimens. This restrictive sampling strategy provides the opportunity to look at the covariation of features from different portions of the skull. The disadvantage is the exclusion of specimens that have been critically discussed in this context, namely Bodo (*H. rhodesiensis*) and the Feldhofer skull cap, the holotype of *H. neanderthalensis*. Independently of this deliberate restriction, there are further limitations that arise from the (in)accessibility of original specimens. When unavailable, casts were used in their stead. Neandertals are represented by the most complete Wuermian specimens currently known (La Chapelle-aux-Saints, La Ferrassie I and Guattari 1). La Quina H5 was excluded due to its preservation. I included the only *H. erectus* skulls with face (Sangiran 17 and KNM-ER 3733), as well as a Sinanthropus composite based on fragments from Zhoukoudian skulls I-III, VI, X, XII, and XIV (Tattersall and Sawyer, 1992). Assignment of Middle Pleistocene hominins to *H. heidelbergensis/rhodesiensis* varies by author, but is assumed by several for Kabwe (holotype of *H. rhodesiensis*), Petralona, Steinheim and the Sima de los Huesos material, of which hominin 5 (SH5) was included in this study. In addition to early anatomically modern fossils from the Near East (Skhul 5, Qafzeh 6) one early Upper Paleolithic modern human (Mladec 1), three randomly chosen modern human crania (from central Europe, East Africa and Greenland) were included in the analyses. Modern humans were limited to three for reasons of sample balance.

3D scan data were post-processed with commercial software and converted to a standard polygon mesh format. Only in the case of Guattari, the surface model was derived from CT data (with a voxel matrix of $512 \times 512 \times 340$). CT data, while increasingly available for fossil hominins, are not an optimal source for quantitative studies of external structures, because they require special protocols in order to yield accurate surface models or linear measurements (Spoor et al., 1993). Because the limit of two tissues (in this case bone to air) can only be determined by finding the median Hounsfield value, which varies among and within specimens, thresholding must reflect these variations, thus

**Table 1**
List of fossils and their presumed taxonomic affiliation. Casts are identified by (c).
**Tableau 1**
Liste de spécimens fossiles et de leur affiliation taxonomique présumée. Les moulages sont identifiés par (c).

| Specimen | Site | Chronology (bp) | *Taxonomy* |
|---|---|---|---|
| La Ferrassie I (o) | La Ferrassie, France | Wuerm, 60–70 000 | |
| Guattari, Italie (o) | Monte Circeo, Italie | Wuerm, 55–60 000 | *H. neanderthalensis* |
| La Chapelle-aux-Saints (o) | La Chapelle-aux-Saints, France | Wuerm, 52 000 | |
| Petralona (c) | Petralona, Grece | 250–400 000 | |
| SH5 (c) | Atapuerca, Espagne | 250–600 000 | *H. heidelbergensis* |
| Steinheim (o) | Steinheim, Allemagne | 300–400 000 | |
| Kabwe (o) | Kabwe, Zambie | 250–600 000 | *H. rhodesiensis* |
| Sangiran 17 (c) | Sangiran, Indonesie | 1–1.3 my bp | |
| Sinanthropus pekinensis (c)[a] | Zoukhoudian, Chine | 680–780 000 | *H. erectus sensu lato* |
| KNM-ER3733 (c) | East-Rudolph, Kenya | 1.8 my | |
| Skhul V (c) | Skhul, Israel | 90–100 000 | |
| Mladec 1 (o) | Mladec, Tchequie | 31 000 | *H. sapiens* |
| Qafzeh 6 (o) | Qafzeh, Israel | 92 000 | |

[a] Reconstruction by Tattersall and Sawyer (1996), courtesy of Dept. Anthropology, AMNH.

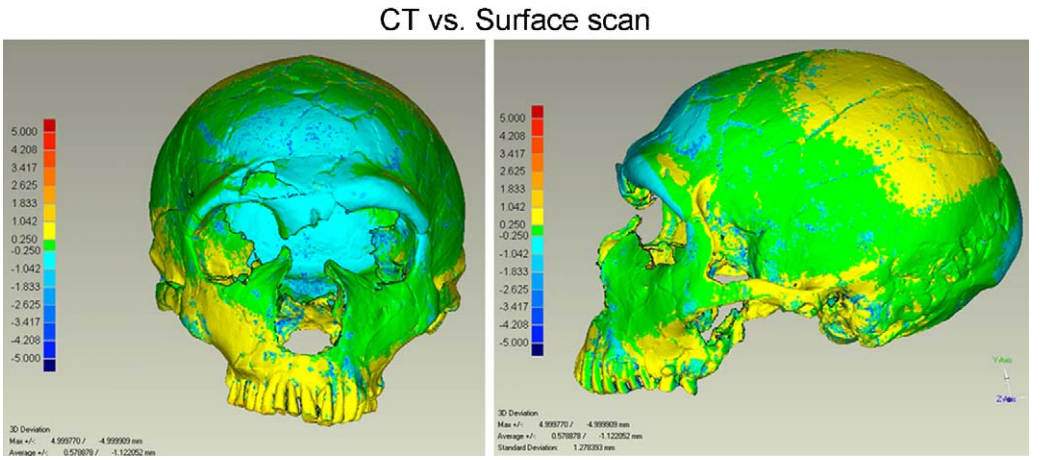


**Fig. 1.** Map of deviations between a surface scan and a model derived through global thresholding from a CT-scan (La Ferrassie I Neandertal).
**Fig. 1.** Cartographie des déviations entre *scan* surfacique et modèle surfacique obtenu à partir d'un CT-*scan* par seuillage global (Néandertalien de La Ferrassie I).

requiring segmentation of each slice (HMH thresholding protocol). Global thresholding on the other hand, i.e. the use of a single Hounsfield range for the entire skull, can result in deviations of several millimeters between the actual bone surface and its estimate (Fig. 1), the impact of which in quantitative analyses has not been fully studied.

For each specimen 24 landmarks and 587 semilandmarks were recorded (Fig. 2) with the software "landmark Editor" (Wiley, 2005), as illustrated by Harcourt-Smith et al. (2008). Table 2 lists the 24 conventional landmarks. The semilandmarks were generated by defining surface patches corresponding as closely as possible to individual bones (i.e. frontal, parietal, temporal, zygomatic, maxilla). Because geometric morphometric analysis requires complete data sets, missing data were estimated either through mirror imaging (bilateral points), or linear regression (sagittal points), or visually in cases of minor damage. In the case of Steinheim, the original left side was completely substituted through mirroring. Fig. 3 shows the result of mirror imaging in the case of Kabwe, which is missing the right zygomatic arch and large portions of the temporal and occipital, whereas the left side is completely preserved. The usability of virtually reconstructed hominins for quantitative analyses has been discussed before (Gunz et al., 2009b).

Landmarks were aligned by generalized Procrustes Analysis (GPA), with semilandmarks being treated as type III landmarks (Maddux and Franciscus, 2009; Niewoehner, 2001). Procrustes residuals were submitted to a Principal Components Analysis (PCA) to explore major directions of shape variation in the sample. Principal components

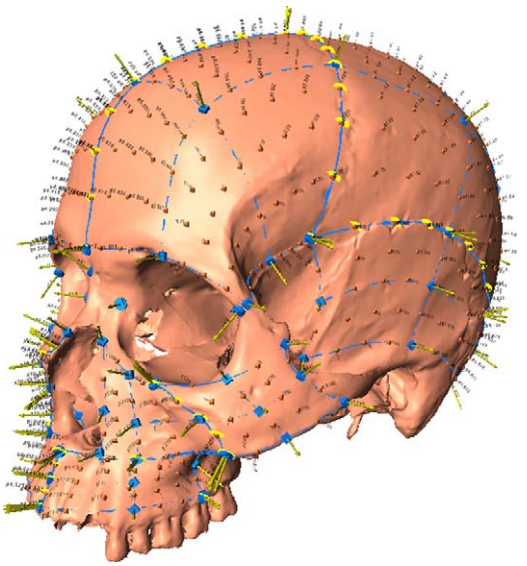

**Fig. 2.** The 587 landmarks and semilandmarks derived from a 3D surface scan, shown on a modern human from East Africa.
**Fig. 2.** Représentation des 587 *landmarks* et *semilandmarks* enregistrés à partir d'un *scan* surfacique d'un homme moderne en provenance de l'Afrique de l'Est.

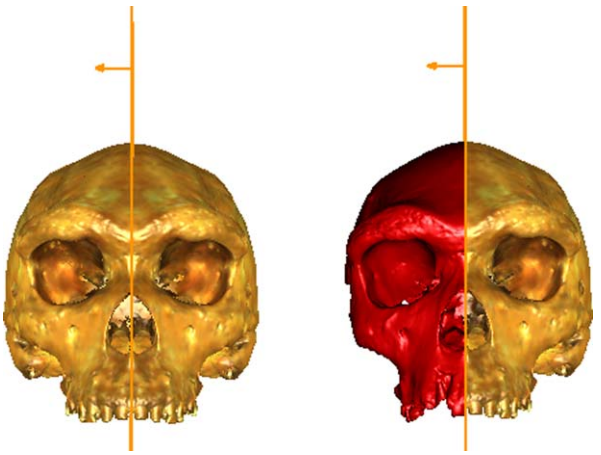

**Fig. 3.** Using the mediansagittal plane to mirror-image missing portions on one side to the other, illustrated for Kabwe.
**Fig. 3.** Reconstitution des parties manquantes d'un côté à l'autre par transfert d'images par effet miroir, illustré pour Kabwe.

**Table 2**
List of landmarks used in the analysis.
**Tableau 2**
Liste des *landmarks* utilisés dans cette analyse.

| | Landmarks | Fossil estimates | Surface patches |
|---|---|---|---|
| 1 | Nasion | | Parietal left |
| 2 | Ektomolare_l | | Parietal right |
| 3 | Lambda | | Occipital squama |
| 4 | Bregma | | Frontal squama left |
| 5 | Glabella | | Frontal squama right |
| 6 | Inion | | Temporal squama left |
| 7 | Opisthion | Guattari, Qafzeh 6, Steinheim | Temporal squama right |
| 8 | Basion | Guattari, Qafzeh 6, Steinheim, Sinanthropus | Alveolar arch right |
| 9 | Hormion | La Ferrassie I, S17 | Zygomatic right |
| 10 | Prosthion | Steinheim | Maxilla right |
| 11 | Nasospinale | | Alveolar arch left |
| 12 | Dakryon_l | La Ferrassie I | Zygomatic right |
| 13 | Frontomalare orbitale_l | | Maxilla left |
| 14 | Zygo-orbitale_l | | |
| 15 | Zygomaxillare_l | | |
| 16 | Pterion_l | | |
| 17 | Asterion_l | | |
| 18 | Frontomalare orbitale_r | | |
| 19 | Dakryon_r | | |
| 20 | Zygo-orbitale_r | | |
| 21 | Zygomaxillare_r | | |
| 22 | Pterion_r | | |
| 23 | Asterion_r | Kabwe | |
| 24 | Ektomolare_r | | |

were then used in a Canonical Variates Analysis (CVA) to further identify and test group differences. Landmark configurations along the directions of interest were estimated by multivariate regression, and visualized by NURBS (non-uniform rational B-splines) surfaces, which were fitted to the semilandmarks to enhance interpretation and readability. Procrustes and Mahalanobis distances where used to construct phenograms in order to assess shape affinities both at individual and species level. GPA, PCA and CVA were performed in MorphoJ (Klingenberg, 2008), NURBS surfaces were generated in Rhino3D.

## 4. Results

Individual scores along the first two principal components, accounting for roughly 50% (33.1% and 16.2%) of the total variance, are plotted in Fig. 4. Three major scatters, corresponding to three species (*H. erectus, H. neanderthalensis, H. sapiens*) can be recognized in this graph. Both fossil and modern *H. sapiens* are grouped together along principal component 1 (PC 1) and are opposed to all non-modern groups (i.e. *H. erectus*, *H. heidelbergensis* and *H. neanderthalensis*), with Kabwe being close to *H. erectus* s.l. PC 2 tends to separate *H. erectus* s.l. from Neandertals. Kabwe maintains a proximity to *H. erectus* along this axis, while *H. heidelbergensis* specimens are spread out between Neandertals on the one end and *H. erectus* on the other. More specifically, Petralona falls closer to *H. erectus*, Steinheim closer to the Neandertals, while SH5 is intermediate between the two. Hence, the first two components provide a good characterization of calvarial shape in the three species, namely *H. erectus*, *H. sapiens*, and *H. neanderthalensis*.

PC 1 describes mostly a vertical expansion of the fronto-parietal region, a reduction in supraorbital and facial projection and postorbital constriction (Fig. 5). The infraorbital region is much more concave toward the modern sample, thus reflecting the distinctly modern canine fossa. Conversely, non-modern specimens are characterized by a long, low vault, low degree of parietal expansion, a strong supraorbital development and postorbital constriction. Facial dimensions are vertically increased and projecting anteriorly. This plesiomorphic state is represented by all non-modern groups (*H. heidelbergensis*, *H. rhodesiensis*, *H. neanderthalensis*); only Steinheim takes an intermediate position on this axis. Shape differences along PC 2 are heavily located in the face, which is generally reduced, narrower and vertically shortened for negative scores (Neandertals), relative to the positive end of the axis represented by *H. erectus* (plus Kabwe and most *H. sapiens*). However, the region around the *apertura piriformis* is more projected anteriorly in Neandertals, which reflects midfacial prognathism/maxillary inflation. The zygomatic is also relatively smaller and less projecting. In addition, the posterior region of the vault is not rounded, but protrudes to form what can be interpreted as an occipital bun (Fig. 5, vertical view). Its presence in Mladec is likely to cause this specimen's position along PC 2. A postorbital constriction is associated with positive scores, which largely represents *H. erectus*. Among fossils with positive scores (*H. erectus*), the calvarium is relatively widened in the lower temporal region (thus pentagonal in posterior view), whereas negative scores lead to a reduced width in that same region. Overall, PC 2 contrasts *H. erectus* and Neandertals, but also characterizes the differences between Kabwe and Steinheim.

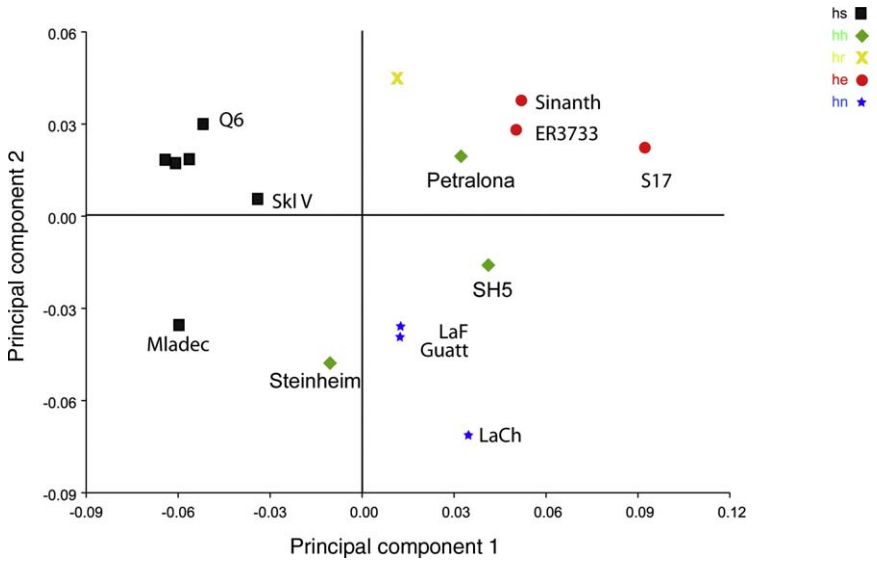


**Fig. 4.** PC scores along axes 1 and 2: *H. sapiens* (squares), *H. erectus* (circles), *H. heidelbergensis* (diamonds), *H. neanderthalensis* (stars), *H. rhodesiensis* (cross).
**Fig. 4.** Scores individuels le long des deux premières composantes principales : *H. sapiens* (carrés), *H. erectus* (cercles), *H. heidelbergensis* (losanges), *H. neanderthalensis* (étoiles), *H. rhodesiensis* (croix).

The shape differences between presumable species are corroborated by a CVA, not displayed here. This analysis yielded significant results (after 10 000 permutations) for the shape difference between *H. erectus* s.l. and *H. sapiens*, as well as between *H. neanderthalensis* and *H. sapiens*, whereas *H. neanderthalensis* and *H. heidelbergensis* were statistically not different. Furthermore, no significant differences were observed for overall size (log centroid size),

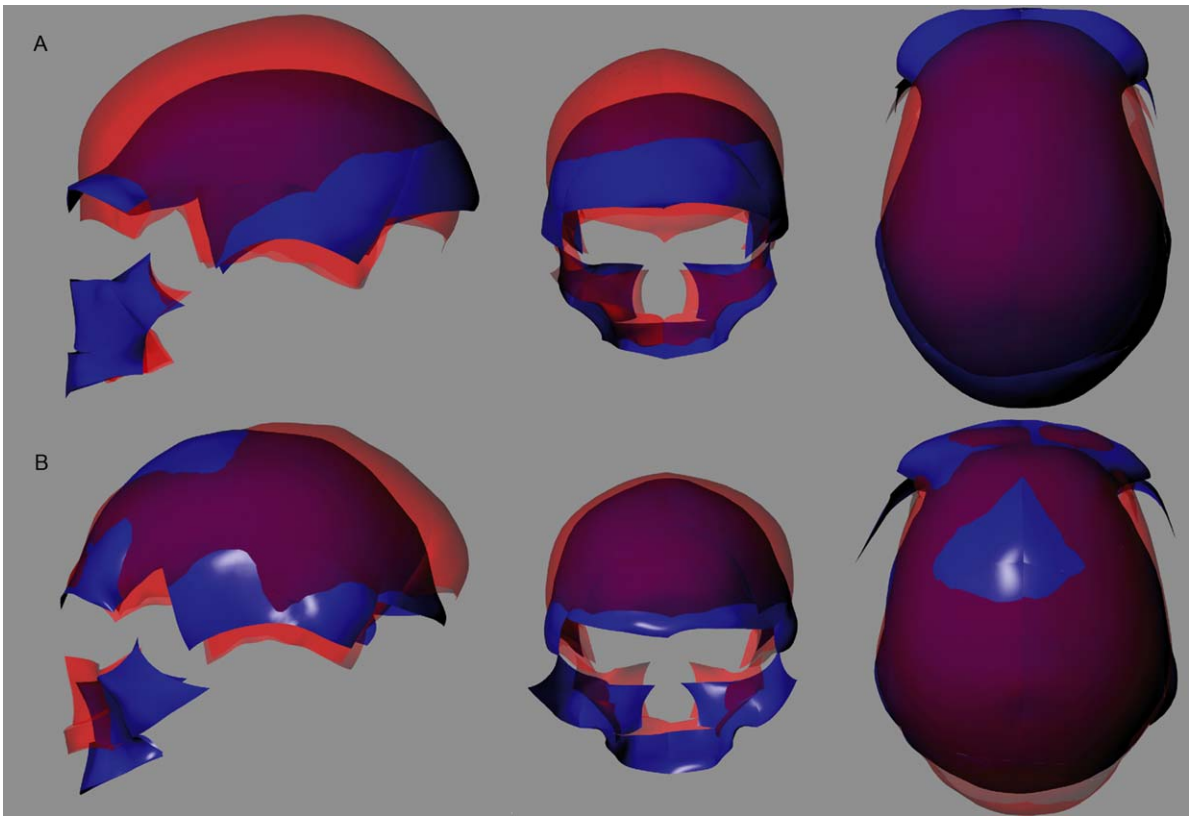


**Fig. 5.** Shape change along principal components 1 (A) and 2 (B). Positive scores in blue, negative scores in red.
**Fig. 5.** Changement de conformation le long des composantes 1 (A) et 2 (B). Scores positifs en bleu, scores négatifs en rouge.

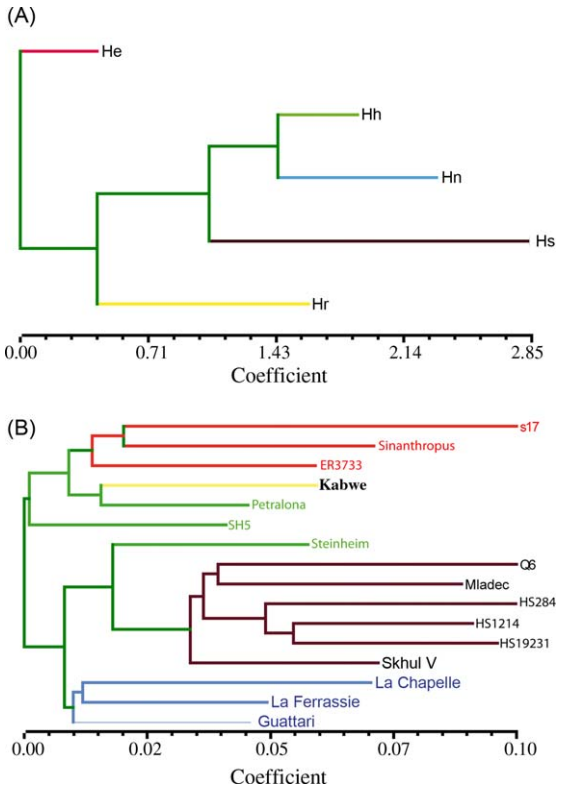


**Fig. 6.** Neighbor-joining trees for species/individuals. A. Mahalanobis distances between species. B. Procrustes distances between specimens.
**Fig. 6.** Arbre phénétique pour espèces/individus par *neighbor-joining*. A. Distance de Mahalanobis entre espèces. B. Distance Procrustes entre individus.

though it is noteworthy that Neandertals showed the least scatter, and their centroid size values were all at the upper end of the range.

Mahalanobis distances were used to compute a neighbor-joining tree (Fig. 6a), which identifies *H. neanderthalensis* and *H. heidelbergensis* as closest, followed by *H. sapiens*, whereas *H. erectus* is farthest, followed by *H. rhodesiensis*. A second neighbor-joining tree was computed from Procrustes distances between individual specimens (Fig. 6b), which is largely consistent with these findings. Thus, three major groups, *H. erectus* s.l., *H. neanderthalensis* and *H. sapiens*, can be distinguished through their calvarial shape, with Kabwe and Petralona closely affiliated with *H. erectus*, while Steinheim is somewhat closer to *H. sapiens/neanderthalensis*.

## 5. Discussion

As was argued by Lieberman et al. (2002), most of the cranial features that characterize *H. sapiens* can be seen as an integrated increase in globularity and reduced facial and supraorbital projection, as well as the appearance of a pronounced canine fossa. Thus, to the extent that these features can be quantified in key fossils, their variation can be interpreted as indicating evolutionary progress towards the modern human shape. Rightmire (2009) uses a similar list of features, to which he adds post-orbital constriction, to identify specimens such as Kabwe (his "Bodo-group") as morphologically more archaic, or not fully modern. Specimens like Skhul and Qafzeh on the other hand are, according to him, sufficiently distinct with respect to these features to justify their inclusion in *H. sapiens*. He argues furthermore that *H. heidelbergensis* retains *erectus*-like plesiomorphies, while displaying *sapiens*-like apomorphic traits, such as an increased cranial capacity, arched temporals, divided supraorbitals and a more vertical nose, making this species ancestral to both modern humans and Neandertals. Gunz et al. (2009a), while not specifically addressing Middle Pleistocene phylogeny, also find that Middle Pleistocene hominins form two distinct morphologies, modern and "archaics" in their terms.

The alternative view (Bermúdez de Castro et al., 1997), assumes that there were two distinct lineages of non-modern hominins during the Middle Pleistocene, only one of which lead to *H. sapiens*, whereas the other lead to Neandertals. Thus, while the question of modern human origins is seen similarly in both views, they differ substantially with respect to Neandertal origins. The fossil specimen from Kabwe, sole representative of African *H. heidelbergensis* / *rhodesiensis*, plays a key role in deciding which scenario is better supported by the data: if it can be distinguished from European Pleistocene forms and if it shares *H. sapiens* apomorphies, it would support the idea of two distinct lineages and an exclusively European origin of Neandertals. This, however, is not the case. Kabwe largely shares a plesiomorphic calvarial shape with *H. erectus* s.l., but fails to score for modern human apomorphies, or Neandertal apomorphies. Calvarial shape alone does not support its claimed ancestry to *H. sapiens*, or to *H. neanderthalensis*. However, all analyses performed here, including the neighbor-joining tree (Fig. 6), stress its calvarial proximity to both Petralona and SH5, two European fossils largely considered to be representatives of *H. heidelbergensis* and close to Neandertals. Whatever the phylogenetic position of Kabwe and Petralona may be, the results shown here corroborate previously reported strong affinities between the two. This can be seen in support of a scenario according to which they belong to the same evolutionary grade or clade, rather than separating them into an African (*H. rhodesiensis*) and a European clade (*H. heidelbergensis*). Grouping them together into the same taxon (i.e. *H. rhodesiensis*) raises the issue of their phylogenetic relation to *H. heidelbergensis* and *H. neanderthalensis*. Hublin (2009) groups *H. rhodesiensis* and *H. heidelbergensis* together, but favors the species name *H. rhodesiensis*. In the absence of clear Neandertal apomorphies pertaining to calvarial shape, they should be considered either as an ancestral or a sister lineage to Neandertals.

Calvarial features that have been described as Neandertal apomorphies (midfacial prognathism, sagittally oriented and inflated infraorbitals, occipital bun) do in fact contribute to their statistical separation from both *H. sapiens* and *H. erectus*. Neandertals are also distinct from *H. erectus* in this analysis because of parietal expansion, a derived feature they share with *H. sapiens*. The results suggest that Steinheim and possibly SH5 share at least the parietal expansion, perhaps even the more coronally oriented infraorbital region. This last character, however, is

subject to a more thorough reconstruction and analysis of the Steinheim skull, which shows some plastic deformation in this area.

Based on significance levels obtained through permutation tests, only three fossil groups can be sufficiently well distinguished on morphometric grounds: *H. erectus* s.l., *H. neanderthalensis*, and *H. sapiens*, whereas the case for distinguishing an "archaic *Homo*" from both Neandertals and *H. erectus* is not strong. Steinheim, with its intermediate position on axis 1 and Neandertal apomorphic traits in the face represents the strongest argument, in this study, for *H. heidelbergensis sensu* Rightmire (1998; 2009), which incidentally would also fit current estimates of the last common genetic ancestor of *H. sapiens* and *neanderthalensis* at around 300–400 ky (Endicott et al., 2010). It must be stressed here, that this study is exploratory, that the number of well-preserved specimens available for studying complete calvarial patterns remains a major constraint, and that further analyses are needed to provide more definitive answers to the Middle Pleistocene muddle. Still, the striking affinities between the holotype of *H. rhodensiensis* (Kabwe) and a European fossil (Petralona), as demonstrated previously and confirmed here, are unlikely to disappear, even if more complete specimens were to be included in the analysis. This makes *H. rhodesiensis* an Afro-European species that retains an *erectus*-like plesiomorphic calvarial shape, but no Neandertal/*H. sapiens* apomorphies, unless one lumps it with SH5 and Steinheim, which together appear to bridge the morphospace between *H. sapiens*, *H. neanderthalensis* and *H. erectus*. In the absence of stronger evidence, such a lumping seems premature.

## 6. Conclusion

The increasing availablility and use of 3D imagery and morphometrics, coupled with current state-of-the-art computing power, opens new areas of investigation in palaeoanthropology, previously not possible. Applying these tools systematically and on a large scale allows for a more accurate quantification of any given morphology, and offers the opportunity to quantify shapes much more comprehensively: With the "revolution in morphometrics" (Rohlf and Marcus, 1993) having reached adulthood, a major constraint, the description of a shape through a reduced subset of points and curves, is about to disappear thanks to the increasing availability of 3D surface data and advanced analytical techniques. When applied to a specific issue in hominin phylogeny, the massive amount of data generated in 3D morphometrics provides quantitative assessments of morphological features that are often described qualitatively, or whose objective measurement proved difficult in the past. Thus, variation of calvarial shape in *H. erectus*, Neandertals and modern humans allows for a statistical separation, which in turn can be used to phylogenetically assess the role of *H. heidelbergensis* and/or *rhodesiensis*. Based on these data, the case for an exclusively African clade (*H. rhodesiensis*) in the Middle Pleistocene, ancestral only to *H. sapiens* is very weak. Alternatively, the close affinity of Kabwe and Petralona to each other and to *H. erectus*. s.l. could either be used as argument for lumping it with this species, or for considering it as an afro-European sister group of a branch that ultimately lead to *H. heidelbergensis*, *H. neanderthalensis* and *H. sapiens*. Defining *H. heidelbergensis,* on the other hand, as ancestral to both *H. sapiens* and *H. neanderthalensis* is conceivable only if specimens such as Steinheim and SH5 are included. Given the post-mortem damage of Steinheim, fully assessing its morphology requires a more detailed reconstructive effort and comparative analysis using geometric morphometrics and virtual imagery. Overall, the results presented here are consistent with the idea of a number of non-modern Middle Pleistocene species in excess of the two commonly identified.

## Acknowledgments

I would like to thank the following individuals for providing access to specimens and scans: Robert Kruszynski, Henri de Lumley, Roberto Macchiarelli, Philippe Mennecier, Chris Stringer, Ian Tattersall, Maria Teschler-Nicola, Gerhard Weber, Reinhard Ziegler. Eric Delson, Scott Maddux and two anonymous reviewers provided helpful comments. This is NYCEP morphometrics contribution number 47.

## References

Bermúdez de Castro, J.L., Arsuaga, J.M., Carbonell, E., Rosas, A., Martínez, I., Mosquera, M., 1997. A Hominid from the Lower Pleistocene of Atapuerca, Spain: possible ancestor to Neandertals. Mod. Hum. Sci. 276, 1392–1395.

Bookstein, F.L., 1991. Morphometric Tools for Landmark data: Geometry and Biology. Cambridge University Press, Cambridge, 435 p.

Butzer, K.W., Isaac, G.L., 1976. International Congress of Anthropological and Ethnological Sciences 9C1. In: After the Australopithecines: stratigraphy, ecology, and culture change in the Middle Pleistocene. Mouton, The Hague, 911 p.

Day, M.H., Stringer, C.B., 1982. A reconsideration of the Omo Kibish remains and the *erectus-sapiens* transition. In: de Lumley, M.A. (Ed.), L'*Homo erectus* et la place de Tautavel parmi les hominidés fossiles. Premier Congrès de L'Institut de Paléontologie Humaine, Nice, pp. 573–594.

Dean, D., Hublin, J.-J., Holloway, R., Ziegler, R., 1998. On the phylogenetic position of pre-Neandertal specimen from Reilingen Germany. J. Hum. Evol. 34, 485–508.

Endicott, P., Ho, S.Y.W., Stringer, C.B., 2010. Using genetic evidence to evaluate palaeoanthropological hypotheses for the timing of Neanderthal and modern Human origins. J. Hum. Evol. 59, 87–95.

Friess, M., 2006. The study of craniofacial growth patterns using 3D laser scanning and geometric morphometrics. In: Corner, B.D., Li, P., Tocheri, M. (Eds.), Three-Dimensional Image Capture and Applications. Proceedings SPIE, vol. 6056, pp. 184–188.

Friess, M., Marcus, L.F., Reddy, D.P., Delson, E., 2002. The use of 3D laser scanning techniques for the morphometric analysis of human facial shape variation. In: Mafart, B., Delingette, H. (Eds.), Proceedings of the XIVth UISPP Congress, 2001, Three-Dimensional Imaging in Paleoanthropology and Prehistoric Archaeology. British Archaeological Reports, S1049. Archaeopress, Oxford, UK, pp. 31–35.

Green, R.E., Krause, J., Briggs, A.W., Maricic, T., Stenzel, U., Kircher, M., Patterson, N., Li, H., Zhai, W., Hsi-Yang Fritz, M., Hansen, N.F., Durand, E.Y., Malaspinas, A.-S., Jensen, J.D., Marques-Bonet, T., Alkan, C., Prüfer, K., Meyer, M., Burbano, H.A., Good, J.M., Schultz, R., Aximu-Petri, A., Butthof, A., Höber, B., Höffner, B., Siegemund, M., Weihmann, A., Nusbaum, C., Lander, E.S., Russ, C., Novod, N., Affourtit, J., Egholm, M., Verna, C., Rudan, P., Brajkovic, D., Kucan, Z., Gusic, I., Doronichev, V.B., Golovanova, L.V., Lalueza-Fox, C., de la Rasilla, M., Fortea, J., Rosas, A., Schmitz, R.W., Johnson, P.L.F., Eichler, E.E., Falush, D., Birney, E., Mullikin, J.C., Slatkin, M., Nielsen, R., Kelso, J., Lachmann, M., Reich, D., Pääbo, S., 2010. A draft sequence of the Neandertal genome. Science 328 (5979), 710–722.

Gunz, P., Bookstein, F.L., Mitteroecker, P., Stadlmayr, A., Seidler, H., Weber, G.W., 2009a. Early modern human diversity suggests subdivided pop-

ulation structure and a complex out-of-Africa scenario. Proc. Natl. Acad. Sci. 106(15), 6094–6098.
Gunz, P., Mitteroecker, P., Neubauer, S., Weber, G.W., Bookstein, F.L., 2009b. Principles for the virtual reconstruction of hominid crania. J. Hum. Evol. 57(1), 48–62.
Harcourt-Smith, W.E.H., Tallman, M., Frost, S.R., Wiley, D.F., Rohlf, F.J., Delson, E., 2008. Analysis of selected hominoid joint surfaces using laser scanning and geometric morphometrics: a preliminary report. In: Sargis, E.J., Dagosto, M. (Eds.), Mammalian Evolutionary Morphology. A Tribute to Frederick S. Szalay. Springer, New York, pp. 373–383.
Hublin, J.J., 2009. The origin of Neandertals. Proc. Natl. Acad. Sci. 106(38), 16022–16027.
Klingenberg, C.P., 2008. MorphoJ. Faculty of Life Sciences, University of Manchester, UK, http://www.flywings.org.uk/MorphoJ_page.htm.
Lieberman, D.E., McBratney, B.M., Krovitz, G., 2002. The evolution and development of the cranial form in *Homo sapiens*. Proc. Natl. Acad. Sci. 99, 1134–1139.
Lyons, P.D., Rioux, M., Patterson, R.T., 2000. Application of a three-dimensional color laser scanner to paleontology. Paleontol. Electron. 3(2), 1–16.
Maddux, S.D., Franciscus, R.G., 2009. Allometric scaling of infraorbital surface topography in *Homo*. J. Hum. Evol. 56(2), 161–174.
Niewoehner, W.A., 2001. Behavioral inferences from the Skhul/Qafzeh early modern human hand remains. Proc. Natl. Acad. Sci. 98, 2979–2984.
Rightmire, G.P., 1998. Human evolution in the Middle Pleistocene: the role of *H. heidelbergensis*. Evol. Anthropol. 6(6), 218–227.
Rightmire, G.P., 2009. Middle and Later Pleistocene hominins in Africa and Southwest Asia. Proc. Natl. Acad. Sci. 106(38), 16046–16050.
Rohlf, F.J., Marcus, L.F., 1993. A revolution in morphometrics. Trends Ecol. Evol. 8(4), 129–132.
Spoor, C.F., Zonneveld, F.W., Macho, G.A., 1993. Linear measurements of cortical bone and dental enamel by computed tomography: applications and problems. Am. J. Phys. Anthropol. 91, 469–484.
Tattersall, I., 1992. Species concepts and species identification in human evolution. J. Hum. Evol. 22, 341–349.
Tattersall, I., Sawyer, G.J., 1996. The skull of "Sinanthropus" from Zhoukoudian China: a new reconstruction. J. Hum. Evol. 31(4), 311–314.
Tocheri, M.W., Razdan, A.R., Williams, C., Marzke, M.W., 2005. A 3D quantitative comparison of trapezium and trapezoid relative articular and nonarticular surface area in modern humans and great apes. J. Hum. Evol. 49(5), 570–586.
Wiley, D.F., 2005. Landmark v 3.0. Institute for Data Analysis and Visualization, University of California, Davis.